



Improving the Stability of CsPbBr₃ Perovskite Nanocrystals by Peroxides Post-treatment

Min Liu¹, Zhichun Li¹, Weilin Zheng¹, Long Kong¹ and Liang Li^{1,2*}

¹ School of Environmental Science and Engineering, Shanghai Jiao Tong University, Shanghai, China, ² Shanghai Institute of Pollution Control and Ecological Security, Shanghai, China

Metal oxides exhibit excellent barrier properties against moisture and oxygen, which are regarded as the powerful candidate for boosting the stability of perovskite nanocrystals (NCs). Here, we develop a simple method to coat perovskite NCs with PbO by peroxides post-treatment. Firstly, the didodecyl dimethyl ammonium sulfide (DDAS) was used to modify the CsPbBr₃ NCs (DDAS-CsPbBr₃), and then sequentially treated with benzoyl peroxide (BPO). By this way, the self-metal source (lead) can be easily oxidized, leading to the quick growth of lead oxide (PbO) on the surface of individual CsPbBr₃ NCs. Under illumination with a 450 nm LED light (175 mW/cm²), the PbO coated CsPbBr₃ NCs maintained at ~90% of the initial intensity for 20 h of operations; in contrast, the emission from the CsPbBr₃ NCs completely quenched.

OPEN ACCESS

Edited by:

Peter Reiss,

Commissariat à l'Energie Atomique et
aux Energies Alternatives (CEA),
France

Reviewed by:

Yang Zhao,

University of Western Ontario, Canada
Dmitry Aldakov,
CEA Grenoble, France

*Correspondence:

Liang Li

liangli117@sjtu.edu.cn

Specialty section:

This article was submitted to
Energy Materials,
a section of the journal
Frontiers in Materials

Received: 23 August 2019

Accepted: 14 November 2019

Published: 29 November 2019

Citation:

Liu M, Li Z, Zheng W, Kong L and Li L
(2019) Improving the Stability of
CsPbBr₃ Perovskite Nanocrystals by
Peroxides Post-treatment.
Front. Mater. 6:306.
doi: 10.3389/fmats.2019.00306

Keywords: nanocrystal, lead halide perovskites, oxidation, metal oxide, photostability

INTRODUCTION

All inorganic cesium lead halide (CsPbX₃, X = Cl, Br, and I) perovskite nanocrystals (NCs) are promising materials for optoelectronic applications (Zhang et al., 2018; Juang et al., 2019; Papagiorgis et al., 2019), especially for light emitting because of their optically tunable band gap and excellent photoluminescence quantum yields (PLQY). In spite of the excellent merits of the perovskite NCs in various fields, the applications of perovskite NCs are impeded by several issues with regard to their stability. Perovskite NCs are highly sensitive to polar solvents due to their inherent ionic nature. Surface ligands and even structural integrity may be lost in the polar solvents, such as ethyl alcohol and water (Kim et al., 2015; Li X. et al., 2017). In addition, environmental stresses, such as light, oxygen, and moisture, could make harmful effects on their performance, because these external conditions accelerate the rates of oxidation and hydration, which lead to the photoluminescence quenching (Zhang and Yin, 2018; Zhang et al., 2018; Wei et al., 2019). Therefore, poor stability under operational conditions remains a great challenge for practical applications (Yang et al., 2016). To date, a variety of strategies have been developed toward stable perovskite NCs. For example, strong binding ligands, such as didodecyl dimethyl ammonium bromide (Li Z. et al., 2017) and 2,2'-Iminodi benzoic acid (Pan J. et al., 2017) were introduced to enhance the stability of perovskite NCs. Incorporation into stable materials, such as silica (Liu et al., 2018), silica/alumina monolith (Li Z. et al., 2017), polymer (Wu et al., 2019), and graphene oxide matrix (Pan A. et al., 2017) are another major direction to stabilize perovskite NCs. Unfortunately, the existing insulating barrier layer and relatively large size of the resultant integrated composites make them not well-suitable for many optoelectronic and bio-imaging applications. As well-known, coating oxide is a powerful approach to improve the stability of conventional quantum dots (QDs). However, the direct growing of oxides on CsPbBr₃ NCs is quite challenging because of the lattice mismatch of two kinds of materials.

Metal, for example, steel or aluminum, which are immersed into the strong oxidizers, such as nitric acid and sulfate acid, a very dense oxidation layer can be formed quickly, which could prevent rusting of steel products and improve its service life by blocking the intrusion of water vapor, oxygen and other corrosive substances (Uhlir and O'Connor, 1955; Jovanovic and Hackerman, 1998; Robin et al., 2008). In the field of QDs, oxidant-hydrogen peroxides have been using to improve the luminescent properties of quantum dots. Lee et al. treated CdS QDs with hydrogen peroxide and formed CdSO₄ on the surface of QDs, which increased the radiation recombination rate of CdS QDs and improved their luminous efficiency (Lee et al., 2012). Klyuev et al. prepared CdS QDs in gelatin, followed by hydrogen peroxide treatment, and found that the QDs size became smaller and CdO appeared on the surface (Klyuev et al., 2017). Liu et al. used hydrogen peroxide as an etchant to prepare QDs of different particle sizes (Liu et al., 2008). Under mild oxidative conditions, the yellow-emitting CdSe QDs (546 nm) can be converted into blue-emitting CdSe QDs (466 nm), which provides a simple and fast method for preparing small-diameter CdSe QDs. However, there is no report that the related oxidant improves the stability of CsPbBr₃ NCs by oxidation.

Inspired by the fact that oxidants promote the formation of oxide protective films on metal surfaces, we treated CsPbBr₃ NCs with oxidizing agents, which is expected to improve their stability. However, hydrogen peroxide is insoluble in the CsPbBr₃ NCs toluene solution. Therefore, it is necessary to select a suitable oxidizing agent, which has good solubility in toluene. Benzoyl peroxide (BPO) is a strong oxidant that contains weak oxygen-oxygen linkages that release reactive oxygen when heated. In the polymerization reaction, polymerization is induced as an initiator (Raeesi et al., 2017). At the same time, low concentrations of BPO solutions are commonly used in clinical medicine, and their oxidative properties can effectively treat acne and powder (Thiboutot et al., 2008). In addition, BPO has good solubility in toluene, and it can form a uniform system with CsPbBr₃ NCs toluene solution, which is beneficial to the oxidation reaction. Therefore, BPO is chosen here as an oxidant to treat CsPbBr₃ NCs, and PbO is formed on the surface, which resists the corrosion of water vapor and oxygen, and endows the CsPbBr₃ NCs with excellent photostability.

MATERIALS AND METHODS

Chemicals

Cesium carbonate (Cs₂CO₃, 98%), lead bromide (PbBr₂, 98%), sodium sulfide nonahydrate (Na₂S·9H₂O, 98%), oleylamine (OAm, 90%), didodecyl dimethylammonium bromide (DDAB, Aladdin, 98%), and 1-octadecene (ODE, Aladdin, 90%) were purchased from Aladdin Reagent Co. Oleic acid (OA, 90%) was purchased from Sigma-Aldrich Co. Benzoyl peroxide (BPO, C₁₄H₁₀O₄, 98%) was purchased from Beijing Bailingwei Technology Co., Ltd. Methyl acetate (98%) was purchased from Sinopharm Chemical Reagent Co., Ltd.

Preparation of Cs-oleate

Ten millimolar Cs₂CO₃, 20 mL OA, and 20 mL ODE were loaded into a 100 mL three-necked flask, then was degassed at 120°C for 30 min. Subsequently, the temperature was raised to 150°C under the N₂ protection and a transparent solution was formed, and then the heat source was removed to allow the temperature of the system to fall to room temperature. The concentration of Cs-oleate (CsOA) was 0.5 mmol/mL, which was stored as a stock solution.

Preparation of CsPbBr₃ Nanocrystals

Two millimolar of PbBr₂, 20 mL of ODE, 5 mL of OA, and 5 mL of OAm were placed in a 100 mL three-necked flask, and the reaction system was dried under vacuum at 120°C for 30 min, during which N₂ was introduced several times. Then, the temperature was raised to 180°C under the N₂ protection state, and a preheated (70°C) 1 mL of CsOA solution was quickly injected immediately after the formation of the transparent solution. After 10 s, the flask was placed in an ice water bath to be cooled. The CsPbBr₃ NCs were extracted and washed with toluene and methyl acetate, and then the CsPbBr₃ NCs were dissolved in 20 mL of toluene and stored as a stock solution. The concentration is about 15 mg/mL.

Preparation of DDAS Solution

0.75 mmol of DDAB and 15 mL of toluene were mixed and then treated with sonication for 20 min, marking as solution A. 0.75 mmol of Na₂S·9H₂O was dissolved into 15 mL of distilled via the similar method, marking as solution B. Then, A solution was mixed with the B solution and sonicated for 0.5 h. The mixed solution was centrifuged at 10,000 rpm for 1 min, and the upper layer of toluene solution was taken to obtain a DDAS solution at a concentration of 0.05 mmol/mL, which was stored as stock solution.

Preparation of BPO Toluene Solution

One millimolar of BPO was added into 10 mL of the toluene, and then was sonicated for 1 h. The BPO toluene solution (0.1 mmol/mL) was obtained.

BPO Peroxidation of DDAS Treatment of CsPbBr₃ NCs

Firstly, the CsPbBr₃ NCs were treated with BPO toluene solution at 70°C for 1 h (DDAS-CsPbBr₃ NCs). Subsequently, the BPO was injected by adjusting the speed of the syringe pump, the amount depended on the concentration of CsPbBr₃ NCs, and the reaction was proceeded at 70°C. After 2 h, the solution was cooled down to room temperature, and then washed three times with methyl acetate and toluene, and stored in toluene (BPO-DDAS-CsPbBr₃).

Photostability Test

The absorbance of NCs was adjusted to 1.8 at 450 nm, and the same volume of solution was added to the closed cuvette. We performed photostability tests of NCs on a blue LED module with 0.175 W/cm² light intensity (peak at 450 nm, Philips

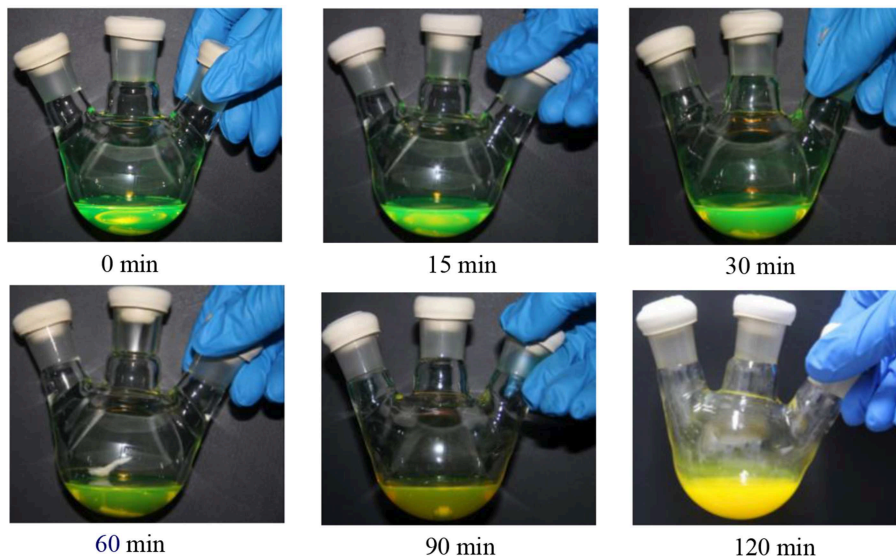


FIGURE 1 | Photographs of CsPbBr₃ NCs and BPO oxidized CsPbBr₃ NCs at different time.

Fortimo). The fluorescence spectrum of the sample was collected at a certain time interval, the PL ratio was obtained by calculating the ratio of the area of the corresponding fluorescence spectrum with the initial fluorescence spectrum.

RESULTS AND DISCUSSION

BPO Direct Peroxidation of CsPbBr₃ NCs

Initially, BPO toluene solution was directly added to a CsPbBr₃ NCs solution using a syringe pump for oxidation. As shown in **Figure 1**, as the reaction time prolonged, the color of the CsPbBr₃ NCs solution gradually changed from green to pale yellow, accompanying by fluorescence quenching (**Figure S1B**). In addition, it was observed that there existed the aggregation of CsPbBr₃ NCs after BPO treatment in the **Figure 2**, which indicated that ligands deriving from the CsPbBr₃ NCs were peeled. Thus, some CsPbBr₃ NCs grew into the larger nanocrystals, which led to the variation of the morphology. Meanwhile, a new phase corresponding to the structure (JCPDS 25-0211) was observed after BPO treatment (**Figure S2**), this phenomenon manifested that CsPbBr₃ NCs underwent the phase change.

BPO Peroxidation DDAS Treated CsPbBr₃ NCs

When BPO was directly applied to oxidize CsPbBr₃ NCs, although photostability is slightly improved (**Figure S1A**), the fluorescence intensity is reduced. Therefore, it is urgent to increase the tolerance of CsPbBr₃ NCs for the BPO. As we known, the unpurified CsPbBr₃ NCs contain a large number of ligands in their solution and have good protection for NCs. Thus, the unpurified CsPbBr₃ NCs were oxidized by BPO and their photostability was tested. As shown in **Figure S3**, the unpurified CsPbBr₃ NCs were oxidized, and their photostability

was improved, but the extent of improvement was very limited. Therefore, it is necessary to further improve the tolerance of CsPbBr₃ NCs for the BPO.

Related literature reported that DDAS could improve the stability of CsPbBr₃ NCs (Li Z. et al., 2017). Therefore, DDAS is used to treat CsPbBr₃ NCs (DDAS-CsPbBr₃) firstly, which improves their resistance to BPO oxidation treatment and maintains excellent photoluminescence of CsPbBr₃ NCs. As shown in **Figure 5**, the fluorescence intensity of CsPbBr₃ NCs was enhanced by DDAS treatment for 1 h (**Figure S4**), which did not affect the fluorescence efficiency of CsPbBr₃ NCs. Subsequently, the BPO toluene solution was injected, and CsPbBr₃ NCs were oxidized at 70°C for 2 h. The solution was cooled down to the room temperature, then purified the BPO oxidized CsPbBr₃ NCs (BPO-DDAS-CsPbBr₃). As shown in **Figure S5**, the fluorescence intensity and peak position of the CsPbBr₃ NCs almost underwent no change during the oxidation process, and the excellent luminescence properties are maintained, and the solution appears bright green (**Figure 3**).

Characterization of BPO-DDAS-CsPbBr₃ NCs

As shown in **Figure 4A**, the BPO-DDAS-CsPbBr₃ NCs showed good photostability. Among them, 0.050 mmol of DDAS treated CsPbBr₃ NCs showed the best photostability after BPO oxidation. After the illumination of 20 h, the fluorescence intensity is 90% of the initial value, while the CsPbBr₃ NCs were almost completely quenched. At the same time, DDAS can also improve the photostability of CsPbBr₃ NCs. In addition, the effect of BPO concentration on the photostability of NCs was investigated. In **Figure 4B**, although 0.125 mmol of BPO treated DDAS-CsPbBr₃ NCs improved their stability, they were much lower than 0.250 mmol of BPO oxidized DDAS-CsPbBr₃ NCs, perhaps due to insufficient oxidation of 0.125 mmol of BPO. In addition,

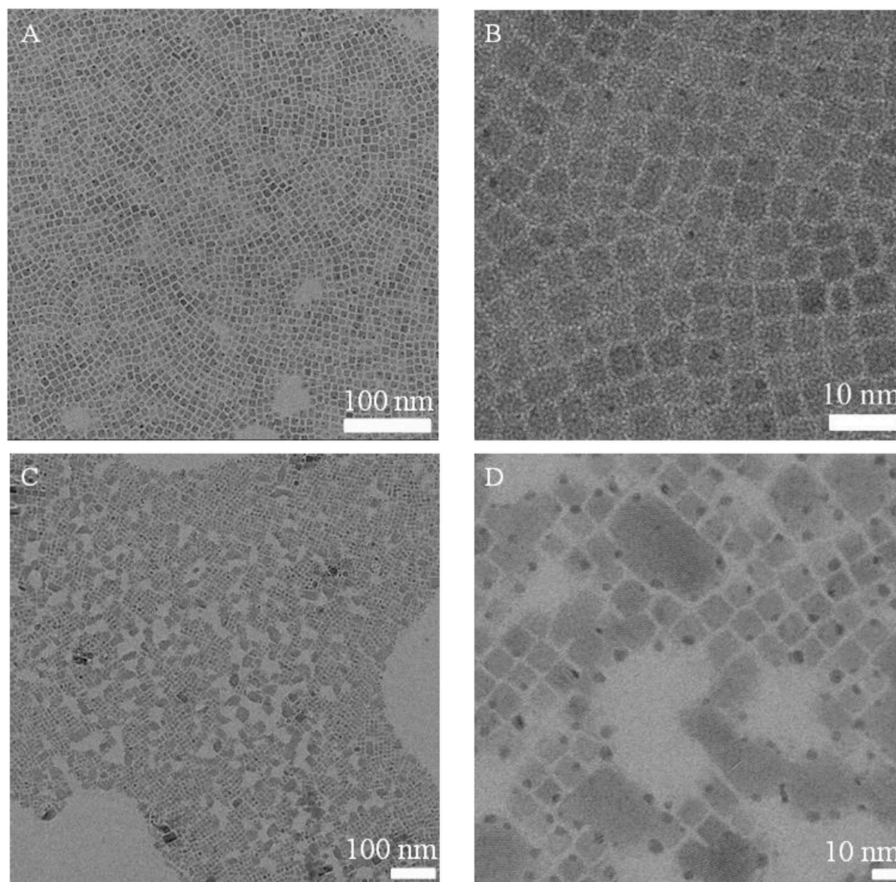


FIGURE 2 | TEM images of CsPbBr₃ NCs (A,B) and BPO oxidized CsPbBr₃ NCs (C,D, 120 min) with different magnifications.



FIGURE 3 | Photographs of CsPbBr₃ NCs, DDAS-CsPbBr₃ NCs, and BPO-DDAS-CsPbBr₃ NCs.

when the BPO was 0.375 mmol, the DDAS-CsPbBr₃ NCs were excessively oxidized; destroying the structure of the NCs, and the solution showed a pale yellow color and became turbid (Figure 5).

At the same time, the morphological changes of CsPbBr₃ NCs were characterized by TEM. As shown in Figure 6, the morphology and size of CsPbBr₃ NCs did not change

significantly after DDAS treatment and BPO oxidation. The average particle size was 8.2, 8.4, and 8.5 nm, respectively. This indicates that the DDAS treatment improves the resistance of CsPbBr₃ NCs for the BPO treatment, and they are not etched by proper BPO during oxidation. The photostability is improved while maintaining the initial morphology and excellent luminescence performance. In addition, we measured the lattice

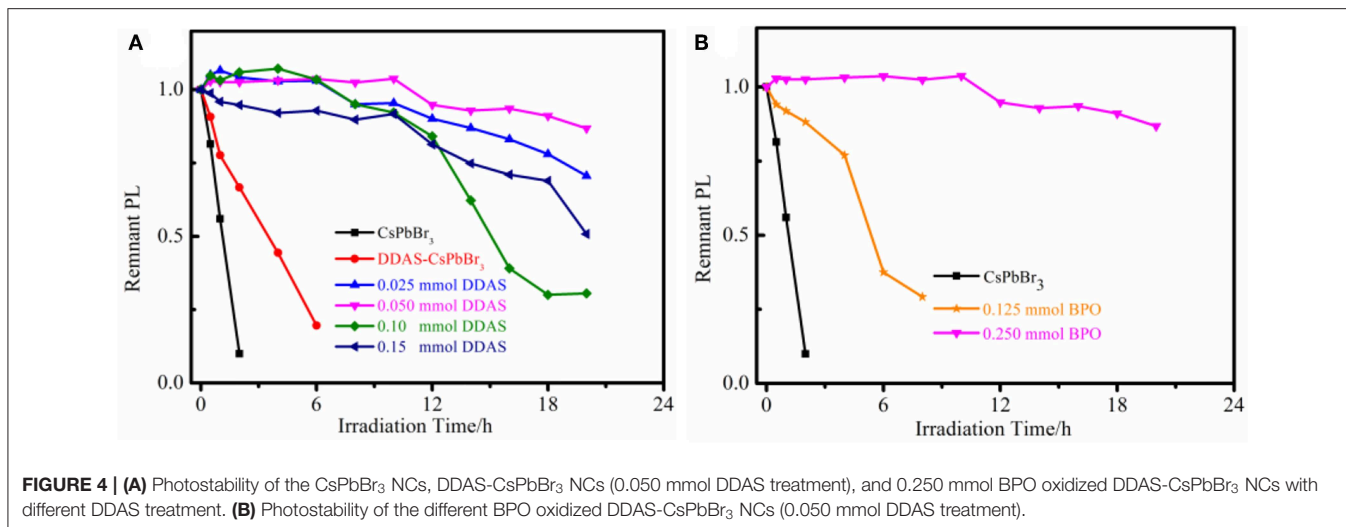


FIGURE 4 | (A) Photostability of the CsPbBr₃ NCs, DDAS-CsPbBr₃ NCs (0.050 mmol DDAS treatment), and 0.250 mmol BPO oxidized DDAS-CsPbBr₃ NCs with different DDAS treatment. **(B)** Photostability of the different BPO oxidized DDAS-CsPbBr₃ NCs (0.050 mmol DDAS treatment).

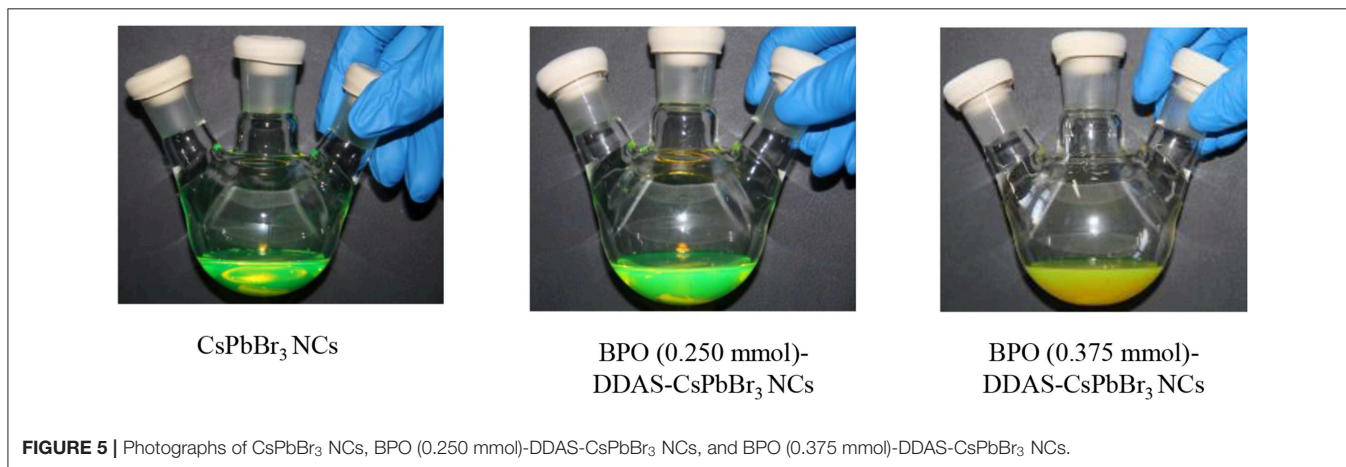


FIGURE 5 | Photographs of CsPbBr₃ NCs, BPO (0.250 mmol)-DDAS-CsPbBr₃ NCs, and BPO (0.375 mmol)-DDAS-CsPbBr₃ NCs.

spacing of the CsPbBr₃ NCs, DDAS-CsPbBr₃ NCs, and BPO-DDAS-CsPbBr₃ NCs. As shown in **Figure S6**, lattice spacing of all the samples is about 0.30 nm corresponding to the (200) crystal faces of the CsPbBr₃ NCs. These results confirm that the BPO treated CsPbBr₃ NCs do not have significant tendency of lattice change. At the same time, the PLQY of CsPbBr₃ NCs is 70%, the DDAS treatment is increased to 81%, and the PLQY of BPO-DDAS-CsPbBr₃ NCs is 78%. It is proved once again that DDAS does improve the tolerance of CsPbBr₃ NCs for the BPO treatment.

In addition, as shown in **Figure S7**, the fluorescence peak position of the BPO-DDAS-CsPbBr₃ NCs is redshifted by 2 nm compared to the CsPbBr₃ NCs. However, as shown in **Figure 6**, the size of CsPbBr₃ NCs are about 8.2 nm, which really exceed in the Bohr radius (Butkus et al., 2017). Therefore, the redshift of the peak position was not caused by the change in the particle size. This may be due to the fact that the electrons or holes of the CsPbBr₃ NCs escape into the formed oxide, resulting in the above phenomenon and the same phenomenon is observed in the CdO-coated CdSe/CdZnS quantum dots (Cho et al., 2017).

The CsPbBr₃ NCs solution, DDAS-CsPbBr₃ NCs solution, and BPO-DDAS-CsPbBr₃ NCs were added dropwise to the quartz glass plate, and then dried to form a film for the XRD test. The spectrum are shown in **Figure 7A**, wherein the (200) crystal plane of the samples were normalized. All the samples corresponded to the cubic perovskite structure (JCPDS 54-0752), with all crystal planes of the perovskite structure appearing, i.e., (100), (110), (200), (210), (211), and (220) crystal planes. Taking the (200) crystal plane as the reference standard, the three samples had similar half-widths, indicating that the particle size of the CsPbBr₃ NCs did not change significantly.

As shown in **Figure 7B**, the FITR of all BPO-DDAS-CsPbBr₃ NCs showed a new absorption peak at 1,023 cm⁻¹ compared to CsPbBr₃ NCs and DDAS-CsPbBr₃ NCs, corresponding to the vibration mode of Pb-O (Alagar et al., 2012; Nouri et al., 2017). It is indicated that PbO is formed on the surface of DDAS-CsPbBr₃ NCs after BPO oxidation, which resists the corrosion of water vapor and oxygen to quantum dots, giving the CsPbBr₃ NCs the excellent photostability. Furthermore, the

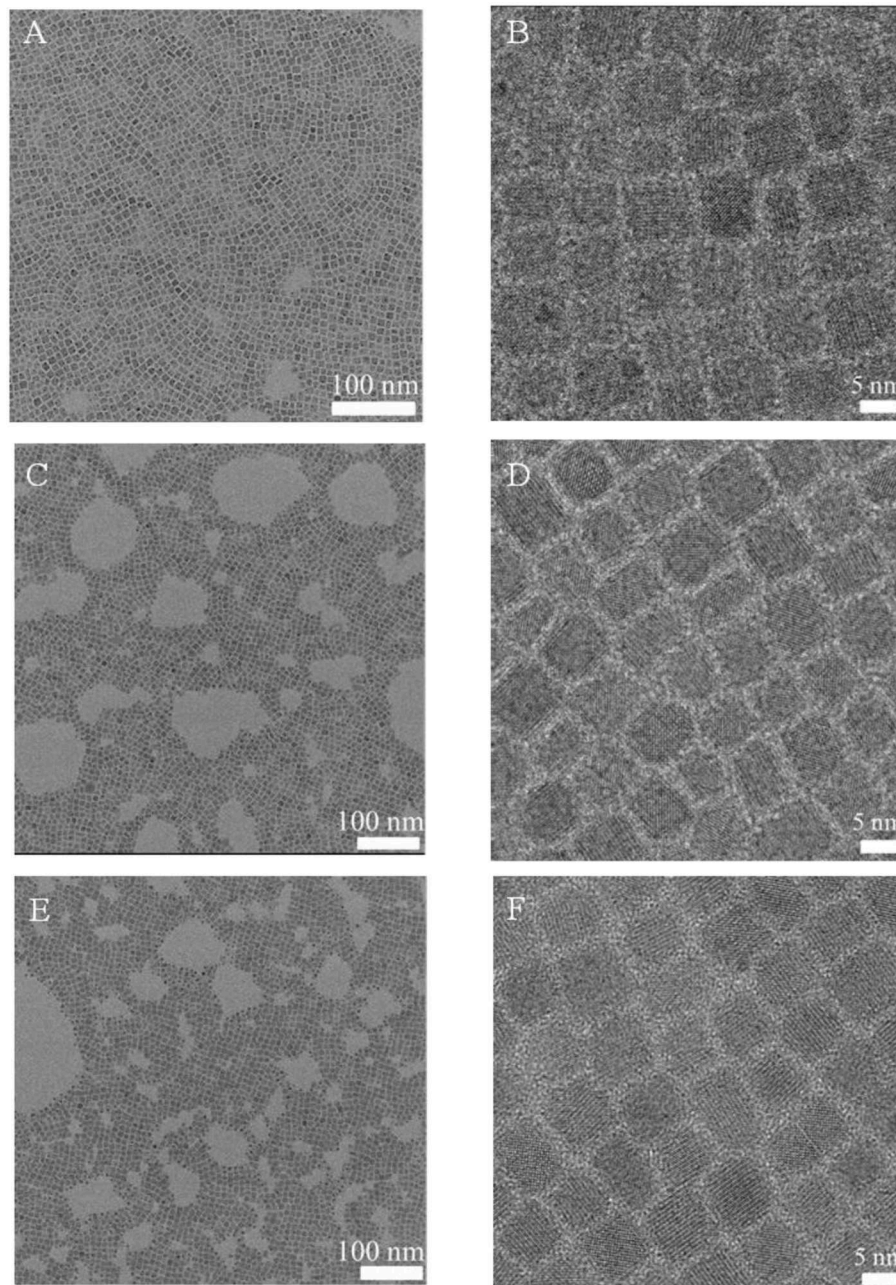


FIGURE 6 | TEM images of CsPbBr₃ NCs (**A,B**), DDAS-CsPbBr₃ NCs (**C,D**), and BPO-DDAS-CsPbBr₃ NCs (**E,F**) with different magnification.

absorption peak at $1,152\text{ cm}^{-1}$ corresponds to the asymmetric stretching vibration mode of SO_4^{2-} (Lane, 2007; Periasamy et al., 2009), which indicates that S^{2-} from the DDAS is oxidized to SO_4^{2-} .

In order to further confirm that PbO is formed on the surface of DDAS-CsPbBr₃ NCs after BPO oxidation, XPS spectra were also performed to analyze the surface change. As shown in **Figure 8A**, the Pb 4f spectra of DDAS-CsPbBr₃ NCs and BPO-DDAS-CsPbBr₃ NCs can be deconvoluted into two peaks,

respectively. The binding energy at 142.9 eV (142.8 eV) and 138.6 eV (138.0 eV) can be assigned to the Pb atoms of CsPbBr₃ NCs (Cai et al., 2018). In addition, the peaks at 143.1 eV and 138.2 eV could be attributed to the presence of Pb-S (Kong et al., 2017), which derived from the DDAS-CsPbBr₃ NCs. The peaks located at 142.9 and 138.1 eV were associated with the Pb-O (Rondon and Sherwood, 1998). But, it is difficult to distinguish from the spectra of Pb-O and the Pb-S, because it seems that their spectra are close to each other. Meanwhile, the peak at 532.1 eV

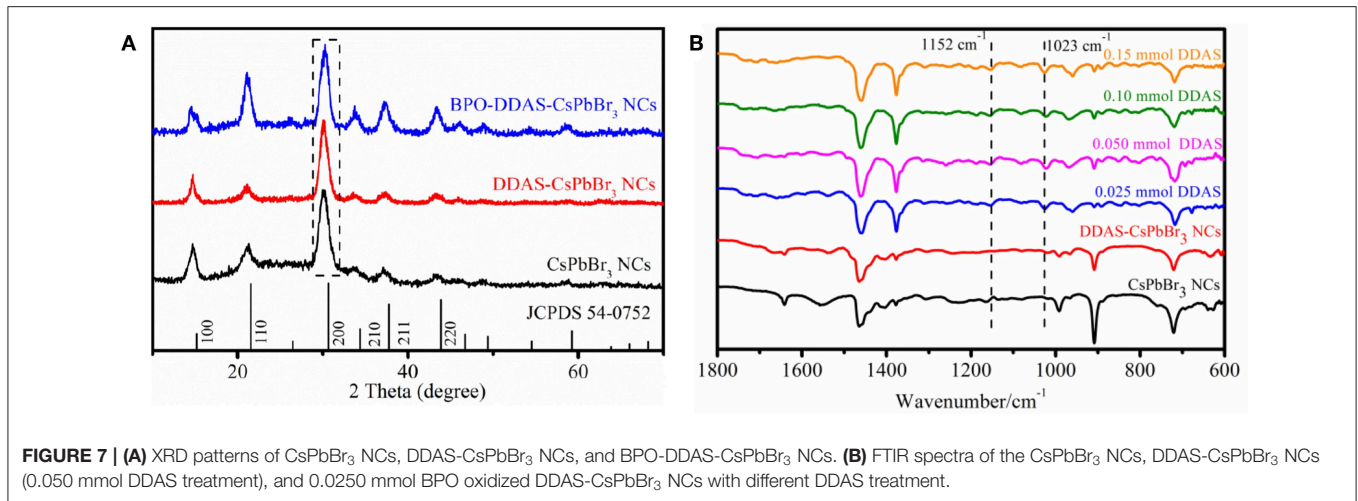


FIGURE 7 | (A) XRD patterns of CsPbBr₃ NCs, DDAS-CsPbBr₃ NCs, and BPO-DDAS-CsPbBr₃ NCs. **(B)** FTIR spectra of the CsPbBr₃ NCs, DDAS-CsPbBr₃ NCs (0.050 mmol DDAS treatment), and 0.0250 mmol BPO oxidized DDAS-CsPbBr₃ NCs with different DDAS treatment.

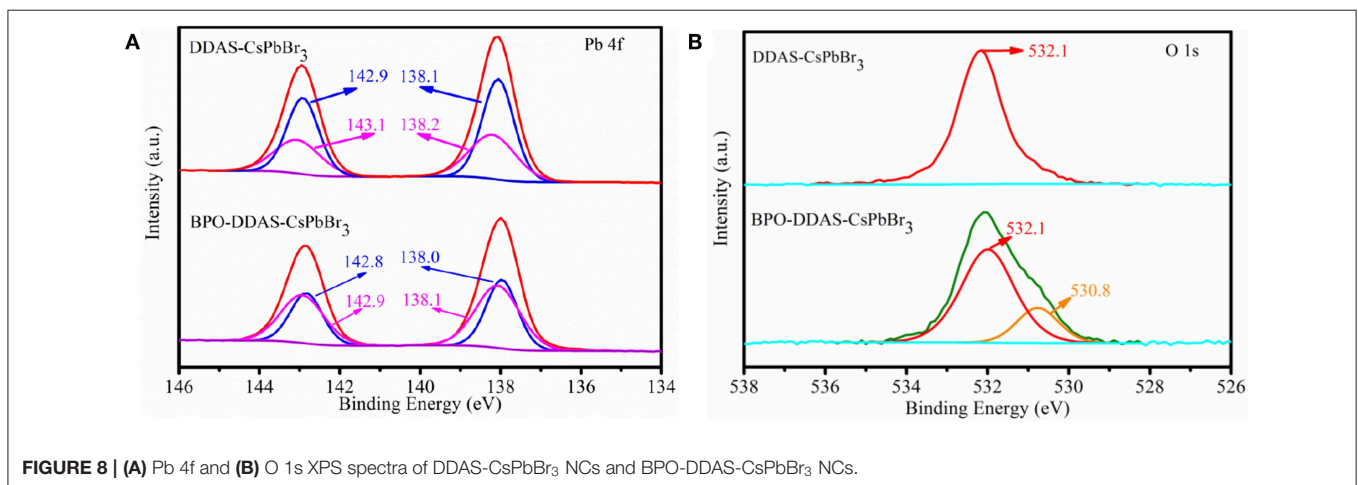


FIGURE 8 | (A) Pb 4f and **(B)** O 1s XPS spectra of DDAS-CsPbBr₃ NCs and BPO-DDAS-CsPbBr₃ NCs.

is assigned to the C=O group arising from the residual OA of the BPO-DDAS-CsPbBr₃ NCs in **Figure 8B** (Zherebetsky et al., 2014). Furthermore, the O 1s peak of BPO-DDAS-CsPbBr₃ NCs was deconvoluted into two peaks with the binding energies of 532.1 and 530.8 eV. The peak at 530.8 eV is possibly attributed to oxygen in the Pb-O of PbO (Huang et al., 2017), which confirmed that the PbO was formed on the surface of DDAS-CsPbBr₃ NCs after BPO oxidation. Therefore, on the basis of aforementioned analyses, it can be concluded that the improved stability of CsPbBr₃ NCs is attributed to the protective layer of PbO.

CONCLUSIONS

In summary, DDAS is firstly used to treat CsPbBr₃ NCs, following by BPO oxidation treatment to generate PbO on the surface of CsPbBr₃ NCs. The compact PbO acts as robust protective layer to prevent the NCs from the attack of oxygen and moisture. Therefore, CsPbBr₃ NCs exhibit stronger photostability under illumination. We believe that this strategy represents a universal approach to improving the stability of NCs in optoelectronic applications.

DATA AVAILABILITY STATEMENT

All datasets generated for this study are included in the article/**Supplementary Material**.

AUTHOR CONTRIBUTIONS

ML and ZL contributed to the CsPbBr₃ NCs synthesis. LK and WZ contributed to the imaging of NCs. LL designed the experiments.

FUNDING

This work was supported by the Guangdong Province's 2018-2019 Key R&D Program (2019B010924001), National Natural Science Foundation of China (NSFC 21773155), and Shanghai Sailing Program (19YF1422200).

SUPPLEMENTARY MATERIAL

The Supplementary Material for this article can be found online at: <https://www.frontiersin.org/articles/10.3389/fmats.2019.00306/full#supplementary-material>

REFERENCES

- Alagar, M., Theivasanthi, T., and Raja, A. K. (2012). Chemical synthesis of nano-sized particles of lead oxide and their characterization studies. *J. Appl. Sci.* 12, 398–401. doi: 10.3923/jas.2012.398.401
- Butkus, J., Vashishtha, P., Chen, K., Gallaher, J. K., Prasad, S. K. K., Metin, D. Z., et al. (2017). The evolution of quantum confinement in CsPbBr₃ perovskite nanocrystals. *Chem. Mater.* 29, 3644–3652. doi: 10.1021/acs.chemmater.7b00478
- Cai, Y., Wang, L., Zhou, T., Zheng, P., Li, Y., and Xie, R. J. (2018). Improved stability of CsPbBr₃ perovskite quantum dots achieved by suppressing interligand proton transfer and applying a polystyrene coating. *Nanoscale* 45, 21441–21450. doi: 10.1039/C8NR06607H
- Cho, J., Jung, Y. K., Lee, J. K., and Jung, H. S. (2017). Surface coating of gradient alloy quantum dots with oxide layer in white-light-emitting diodes for display backlights. *Langmuir* 33, 13040–13050. doi: 10.1021/acs.langmuir.7b03335
- Huang, S., Li, Z., Wang, B., Zhu, N., Zhang, C., and Kong, L. (2017). Morphology evolution and degradation of CsPbBr₃ nanocrystals under blue light-emitting diode illumination. *ACS Appl. Mater. Interfaces* 8, 7249–7258. doi: 10.1021/acsami.6b14423
- Jovanovic, V. M., and Hackerman, N. (1998). Electrochemical passivation of iron in NO₃⁻, SO₄²⁻, and ClO₄⁻ Solutions. *J. Phys. Chem. B* 102, 9855–9860. doi: 10.1021/jp982602z
- Juang, S. S., Lin, P. Y., Lin, Y. C., Chen, Y. S., Shen, P. S., Guo, Y. L., et al. (2019). Energy harvesting under dim-light condition with dye-sensitized and perovskite solar cells. *Front. Chem.* 7:209. doi: 10.3389/fchem.2019.00209
- Kim, Y., Yassitepe, E., Voznyy, O., Comin, R., Walters, G., Gong, X., et al. (2015). Efficient luminescence from perovskite quantum dot solids. *ACS Appl. Mater. Interfaces* 7, 25007–25013. doi: 10.1021/acsami.5b09084
- Klyuev, V. G., Volykhin, D. V., and Ivanova, A. A. (2017). Influence of hydrogen peroxide on the stability and optical properties of CdS quantum dots in gelatin. *J. Lumin.* 183, 519–524. doi: 10.1016/j.jlumin.2016.11.069
- Kong, L., Li, Z., Huang, X., Huang, S., Sun, H., Liu, M., et al. (2017). Efficient removal of Pb (II) from water using magnetic Fe₃S₄/reduced graphene oxide composites. *J. Mater. Chem. A* 36, 19333–19342. doi: 10.1039/C7TA05389D
- Lane, M. D. (2007). Mid-infrared emission spectroscopy of sulfate and sulfate-bearing minerals. *Am. Mineral.* 92, 1–18. doi: 10.2138/am.2007.2170
- Lee, W., Kim, H., Jung, D. R., Kim, J., Nahm, C., Lee, J., et al. (2012). An effective oxidation approach for luminescence enhancement in CdS quantum dots by H₂O₂. *Nanoscale Res. Lett.* 7:672. doi: 10.1186/1556-276X-7-672
- Li, X., Cao, F., Yu, D., Chen, J., Sun, Z., Shen, Y., et al. (2017). All inorganic halide perovskites nanosystem: synthesis, structural features, optical properties and optoelectronic applications. *Small* 13:1603996. doi: 10.1002/smll.201603996
- Li, Z., Kong, L., Huang, S., and Li, L. (2017). Highly luminescent and ultrastable CsPbBr₃ perovskite quantum dots incorporated into a silica/alumina monolith. *Angew. Chem. Int. Ed.* 56, 8134–8138. doi: 10.1002/anie.201703264
- Liu, L., Peng, Q., and Li, Y. (2008). An effective oxidation route to blue emission CdSe quantum dots. *Inorg. Chem.* 47, 3182–3187. doi: 10.1021/ic702203c
- Liu, Z., Zhang, Y., Fan, Y., Chen, Z., Tang, Z., Zhao, J., et al. (2018). Toward highly luminescent and stabilized silica-coated perovskite quantum dots through simply mixing and stirring under room temperature in air. *ACS Appl. Mater. Interfaces* 10, 13053–13061. doi: 10.1021/acsami.7b18964
- Nouri, M., Alizadeh, P., and Tavooosi, M. (2017). The relationship between structural and optical properties of GeO₂-PbO glasses. *J. Adv. Mater. Process.* 5, 3–10.
- Pan, A., Jurow, M. J., Qiu, F., Yang, J., Ren, B., Urban, J. J., et al. (2017). Nanorod superstructures from a ternary graphene oxide-polymer-csPbX₃ perovskite nanocrystal composite that display high environmental stability. *Nano Lett.* 17, 6759–6765. doi: 10.1021/acs.nanolett.7b02959
- Pan, J., Shang, Y., Yin, J., De Bastiani, M., Peng, W., Dursun, I., et al. (2017). Bidentate ligand-passivated CsPbI₃ perovskite nanocrystals for stable near-unity photoluminescence quantum yield and efficient red light-emitting diodes. *J. Am. Chem. Soc.* 140, 562–565. doi: 10.1021/jacs.7b10647
- Papagiorgis, P. G., Manoli, A., Alexiou, A., Karacosta, P., Karagiorgis, X., Papaparaska, G., et al. (2019). Robust hydrophobic and hydrophilic polymer fibers sensitized by inorganic and hybrid lead halide perovskite nanocrystal emitters. *Front. Chem.* 7:87. doi: 10.3389/fchem.2019.00087
- Periasamy, A., Muruganand, S., and Palaniswamy, M. (2009). Vibrational studies of Na₂SO₄, K₂SO₄, NaHSO₄ and KHSO₄ crystals. *Rasayan J. Chem.* 2, 981–989.
- Raeesi, M., Mirabedini, S. M., and Farnood, R. R. (2017). Preparation of microcapsules containing benzoyl peroxide initiator with gelatin-gum arabic/polyurea-formaldehyde shell and evaluating their storage stability. *ACS Appl. Mater. Interfaces* 9, 20818–20825. doi: 10.1021/acsami.7b03708
- Robin, R., Miserque, F., and Spagnol, V. (2008). Correlation between composition of passive layer and corrosion behavior of high Si-containing austenitic stainless steels in nitric acid. *J. Nucl. Mater.* 375, 65–71. doi: 10.1016/j.jnucmat.2007.10.016
- Rondon, S., and Sherwood, P. M. (1998). Core level and valence band spectra of PbO by XPS. *Surf. Sci. Spectra* 2, 97–103. doi: 10.1116/1.1247866
- Thiboutot, D., Zaenglein, A., Weiss, J., Webster, G., Calvarese, B., and Chen, D. (2008). An aqueous gel fixed combination of clindamycin phosphate 1.2% and benzoyl peroxide 2.5% for the once-daily treatment of moderate to severe acne vulgaris: assessment of efficacy and safety in 2813 patients. *J. Am. Acad. Dermatol.* 59, 792–800. doi: 10.1016/j.jaad.2008.06.040
- Uhlig, H. H., and O'Connor, T. L. (1955). Nature of the passive film on iron in concentrated nitric acid. *J. Electrochem. Soc.* 102, 562–572. doi: 10.1149/1.2429913
- Wei, Y., Cheng, Z., and Lin, J. (2019). An overview on enhancing the stability of lead halide perovskite quantum dots and their applications in phosphor-converted LEDs. *Chem. Soc. Rev.* 48, 310–350. doi: 10.1039/C8CS00740C
- Wu, H., Wang, S., Cao, F., Zhou, J., Wu, Q., Wang, H., et al. (2019). Ultrastable inorganic perovskite nanocrystals coated with a thick long-chain polymer for efficient white light-emitting diodes. *Chem. Mater.* 31, 1936–1940. doi: 10.1021/acs.chemmater.8b04634
- Yang, G., Fan, Q., Chen, B., Zhou, Q., and Zhong, H. (2016). Re-precipitation synthesis of luminescent CH₃NH₃PbBr₃/NaNO₃ nanocomposites with enhanced stability. *J. Mater. Chem. C*, 4, 11387–11391. doi: 10.1039/C6TC04069A
- Zhang, F., Xiao, C., Li, Y., Zhang, X., Tang, J., Chang, S., et al. (2018). Gram-scale synthesis of blue-emitting CH₃NH₃PbBr₃ quantum dots through phase transfer strategy. *Front. Chem.* 6:444. doi: 10.3389/fchem.2018.00444
- Zhang, Q., and Yin, Y. (2018). All-inorganic metal halide perovskite nanocrystals: opportunities and challenges. *ACS Cent. Sci.* 4, 668–679. doi: 10.1021/acscentsci.8b00201
- Zherebetskyy, D., Scheele, M., Zhang, Y., Bronstein, N., Thompson, C., Britt, D., et al. (2014). Hydroxylation of the surface of PbS nanocrystals passivated with oleic acid. *Science* 6190, 1380–1384. doi: 10.1126/science.1252727

Conflict of Interest: The authors declare that the research was conducted in the absence of any commercial or financial relationships that could be construed as a potential conflict of interest.

Copyright © 2019 Liu, Li, Zheng, Kong and Li. This is an open-access article distributed under the terms of the Creative Commons Attribution License (CC BY). The use, distribution or reproduction in other forums is permitted, provided the original author(s) and the copyright owner(s) are credited and that the original publication in this journal is cited, in accordance with accepted academic practice. No use, distribution or reproduction is permitted which does not comply with these terms.